Journal of Thermal Analysis and Calorimetry, Vol. 96 (2009) 2, 347–351

HYDROGEN IN AMORPHOUS $TM_{33}Zr_{67}$ (*TM*=Fe, Co, Ni) ALLOYS

*Tzveta Himitliiska and T. Spassov**

Department of Chemistry, University of Sofia 'St.Kl.Ohridski', 1 J. Bourchier str., 1164 Sofia, Bulgaria

Hydrogen sorption properties and some corresponding changes in the crystallization of amorphous $TM_{33}Zr_{67}$ (*TM*=Fe, Co, Ni) alloys have been investigated. Relatively large amount of hydrogen was found to dissolve into the amorphous alloys during electrochemical hydrogen charging. The microstructural evolution during annealing of H-charged $Ni_{33}Zr_{67}$ was studied as well. The weaker bonded hydrogen desorbs in a large temperature range (440–625 K) before the crystallization of the amorphous alloys to start. A hydride phase (ZrH_2) was found to form during annealing the H-charged amorphous $Ni_{33}Zr_{67}$ alloy. During heating at constant heating rate the hydride decomposes at about 715 K and formation of Zr_2Ni immediately takes place. The final microstructure of the Zr_2Ni, crystallized from the H-charged matrix, is noticeably finer compared to the material crystallized from the H-free amorphous alloy, most probably due to the higher temperature of Zr_2Ni formation in the H-charged amorphous alloy than in the H-free sample.

Keywords: *amorphous, crystallization, hydrogenation, microstructure, zirconium alloys*

Introduction

Some of the most common materials for hydrogen storage are based on transition metals. The hydrogen storage capacity in metals and alloys is determined by the chemical interactions between the metal and hydrogen atoms as well as by the type, size and number of potential interstitial sites [1]. Amorphous alloys, consisting of a combination of early and late transition metals (LTM/ETM), were found to be very interesting, regarding their interaction with hydrogen [1–4]. Crystallization of Zr-based glasses under certain conditions results in nanocrystalline microstructures [5–8].

Zirconium-containing glasses and nanocrystalline alloys were found to be very interesting for hydrogen storage [9–12]. Quasicrystalline Ti–Zr–Ni [13] and amorphous and quasicrystalline Zr–Cu–Ni–Al alloys [14] were reported to absorb relatively high amounts of hydrogen. Palladium coating was found to significantly enhance the hydrogen absorption/desorption behavior of Zr-based amorphous and quasicrystalline alloys, due to efficient preventing surface oxide layer formation [15]. The heat capacity of $HfH_{1.83}$ was found to be larger than that of pure hafnium as well as depending on the content of hydrogen in HfH_x anomalies of the heat capacity and electrical conductivity were found to result from the phase transitions in the hafnium hydride lattice [16]. On the other hand, hydrogen treatment of materials, incl. H-induced phase transformations, is a promising approach for producing refined microstructures with attractive properties [12, 17–21].

In this work, we investigated the electrochemical hydrogenation and some corresponding changes in the thermal stability and microstructure of amorphous $TM_{33}Zr_{67}$ (*TM*=Ni, Co, Fe) alloys.

Experimental

Amorphous $Ni_{33}Zr_{67}$, $Fe_{33}Zr_{67}$ and $Co_{33}Zr_{67}$ ribbons were prepared by melt spinning under argon atmosphere, as described elsewhere [5]. Cathodic hydrogenation was carried out in a 2:1 glycerin–phosphoric acid electrolyte at 25°C and current density of i=5 mA cm^{-2}. Mechanical polishing of the amorphous ribbons before hydrogen charging was applied. The microstructure of the sample before and after hydriding was characterized by X-ray diffraction (XRD) using CuK_α radiation. The thermal behavior was studied by differential scanning calorimetry (DSC 7, Perkin-Elmer) under Ar atmosphere. The hydrogen content was measured by termogravimetric analysis (TG 2C, Perkin-Elmer).

Results and discussion

The XRD analysis revealed that all as-quenched alloys were in fully amorphous state. Figure 1 shows two amorphous halos for the materials studied – the first one around 37° and a second one around 65° (2Θ). The position of the main diffraction peaks maximums for the different alloys is practically the

* Author for correspondence: tspassov@chem.uni-sofia.bg

1388–6150/$20.00

Akadémiai Kiadó, Budapest, Hungary
Springer, Dordrecht, The Netherlands

same, indicating that the average interatomic distance in the amorphous alloys does not differ noticeably.

The amorphous $TM_{33}Zr_{67}$ (*TM*=Fe, Co, Ni) ribbons were electrochemically charged with hydrogen. XRD of the hydrogenated materials shows that they are still amorphous (Fig. 2). The diffraction peaks intensities, however, are reduced as a result of the hydrogenation. Any indication for the formation of crystalline phases was not observed. The broad diffraction halo of the amorphous alloys slightly shifts to smaller angels, most probably as a result of the increased distance between the metallic atoms caused by the hydrogen dissolved.

To determine the amount of the absorbed hydrogen and to obtain information about the H-desorption rate a thermogravimetric analysis of the H-charged ribbons at constant heating rate was carried out. Figure 3a reveals that hydrogen charging for 1 h at different current densities in the range

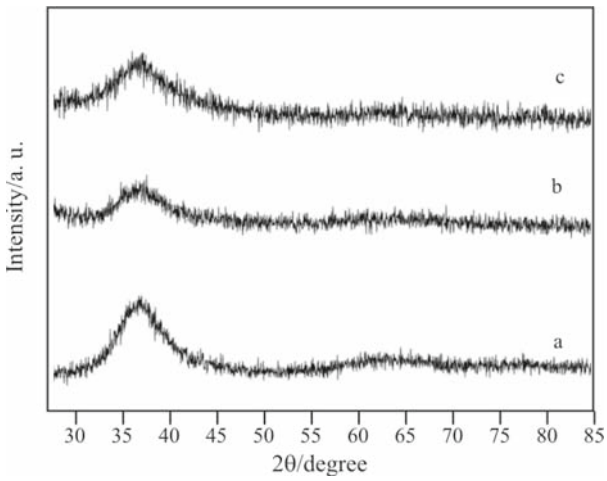

Fig. 1 X-ray diffraction patterns of as-cast amorphous a – $Ni_{33}Zr_{67}$, b – $Fe_{33}Zr_{67}$ and c – $Co_{33}Zr_{67}$ ribbons

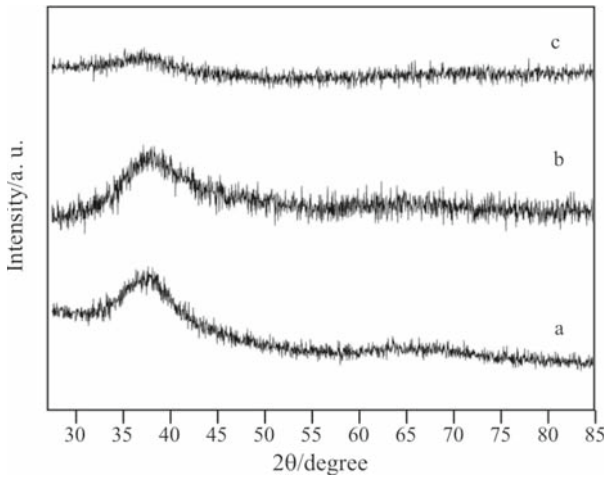

Fig. 2 X-ray diffraction patterns of electrochemically H-charged ribbons: a – $Ni_{33}Zr_{67}$, b – $Fe_{33}Zr_{67}$ and c – $Co_{33}Zr_{67}$

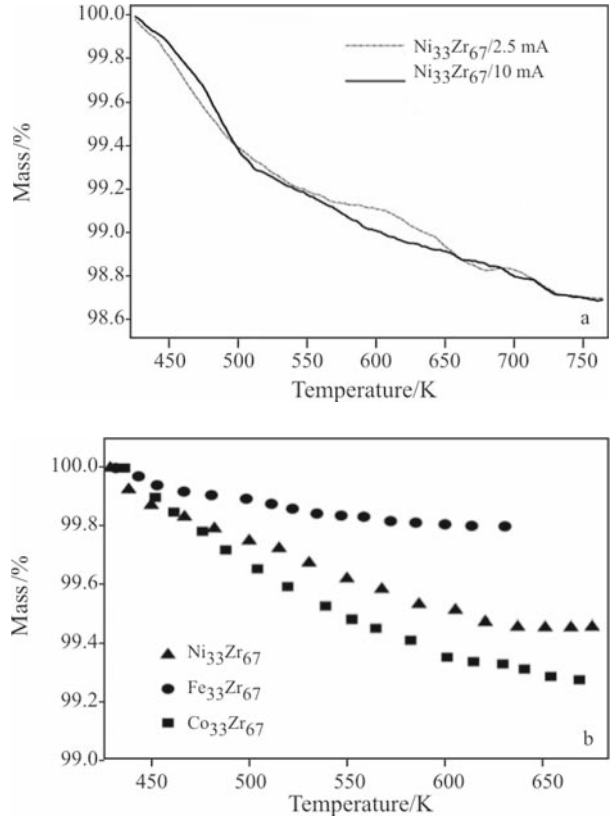

Fig. 3 Hydrogen desorption curves of H-charged amorphous a – $Ni_{33}Zr_{67}$ with two different current densities and b – $TM_{33}Zr_{67}$ (*TM*=Ni, Fe, Co)

2.5–10 mA cm^{-2} results in similar amounts of hydrogen, desorbing in wide temperature range. Comparing the H-desorption curves of the three alloys charged under the same conditions (1 h at 5 mA cm^{-2}) similar amounts of hydrogen, desorbed in the range 440–625 K, are determined for $Ni_{33}Zr_{67}$ and $Co_{33}Zr_{67}$ and a noticeably smaller one for $Fe_{33}Zr_{67}$, Fig. 3b. The process starts at about 440 K, as the amount of hydrogen desorbed is in the range 0.2-0.7 mass% for the different amorphous alloys. These temperatures are below the crystallization temperatures of the H-free amorphous alloys. At this stage we are not able to explain the different H-sorption behavior of $Fe_{33}Zr_{67}$ compared to the other amorphous alloys studied. This question needs to be additionally analyzed.

DSC measurements of the metallic glasses investigated are presented in Fig. 4. The calorimetric curve of the amorphous $Ni_{33}Zr_{67}$ shows a two-step crystallization reaction, as the crystallization product is the tetragonal $NiZr_2$ phase. The two crystallization peaks are partially overlapped and are connected with the same crystallization product. In $Fe_{33}Zr_{67}$, the crystallization reaction is expressed by a single exothermic peak at 675 K and leads to the tetragonal $FeZr_2$ phase. The DSC of $Co_{33}Zr_{67}$ shows single exothermic crystallization peak at 713 K. The DSC analysis reveals

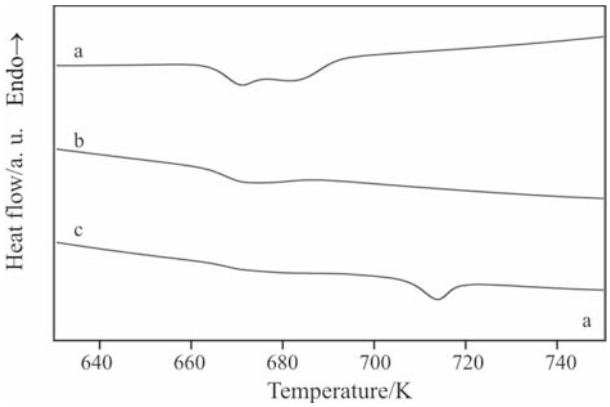

Fig. 4a DSC scans of a – H-free, b – hydrogenated and c – hydrogenated (with larger amount of hydrogen) $Ni_{33}Zr_{67}$

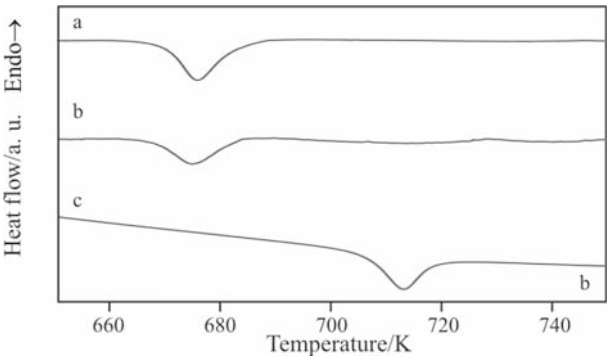

Fig. 4b DSC of a – H-free, b – hydrogenated and c – hydrogenated (with larger amount of hydrogen) $Fe_{33}Zr_{67}$

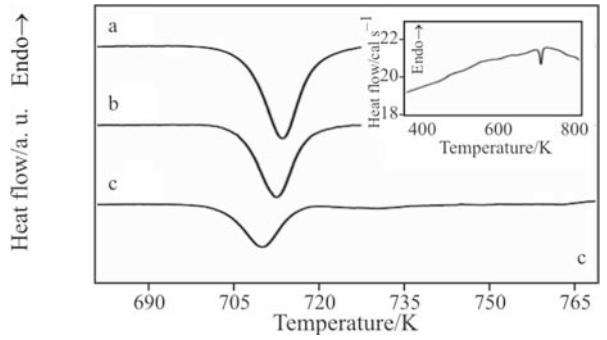

Fig. 4c DSC of a – H-free, b – hydrogenated and c – hydrogenated (with larger amount of hydrogen) $Co_{33}Zr_{67}$. DSC of H-charged $Co_{33}Zr_{67}$ in the larger temperature range (inset)

different thermal stability of the three materials, as the most stable is $Co_{33}Zr_{67}$. For the last alloy the exothermic peak corresponds to the transformation of the amorphous material into the metastable cubic $CoZr_2$ phase, which transforms to the equilibrium tetragonal $CoZr_2$ at higher temperatures [8]. The thermal behavior of the amorphous (Co, Ni, Fe)$_{33}Zr_{67}$ alloys after electrochemical H-charging was studied as well, Fig. 4. Noticeable differences in the calorimetric curves can be seen after hydriding the as-quenched alloys, i.e. the hydrogenation causes changes in the crystallization of the amorphous materials. Figure 4 reveals DSC scans of H-free and charged with different amount of hydrogen $TM_{33}Zr_{67}$ ribbons. Lower hydrogen content of the amorphous $Ni_{33}Zr_{67}$ alloy results in slight decrease of the thermal stability and in overlapping of the two crystallization peaks and then, at higher hydrogen concentrations, in vanishing of the crystallization peaks and appearance of an exothermic peak at higher temperatures (Fig. 4a). The curve of the maximum hydrogenated material shows that the two exothermic peaks in the range 663–693 K almost disappear and a new exothermic peak appears at 713 K. Increasing the amount of hydrogen in the amorphous $Fe_{33}Zr_{67}$ and $Co_{33}Zr_{67}$ results also in continuous decrease of the temperature and enthalpy of crystallization (Fig. 4b and c). At certain hydrogen concentration the exothermic peak of $Fe_{33}Zr_{67}$ shifts to higher temperatures (from ~675K to ~715K), similar to $Ni_{33}Zr_{67}$. It is interesting to be mentioned that the crystallization peak of the $Co_{33}Zr_{67}$ does not shift to higher temperatures even at high hydrogen concentrations in the amorphous alloy (Fig. 4c, inset). For all three alloys the multi-step hydrogen desorption process, registered by TG in the temperature range 440–640°C is also visible on the DSC curves, expressed by several partially overlapped broad endothermic effects, Fig. 4c (inset).

To clarify the nature of the crystallization peak shift to higher temperatures for two of the amorphous alloys studied ($Fe_{33}Zr_{67}$ and $Ni_{33}Zr_{67}$) a XRD analysis of hydrogenated and then annealed in DSC up to different temperatures (before and after the calorimetric peak) $Ni_{33}Zr_{67}$ alloys was carried out (Fig. 5). Mainly ZrH_2 was detected just before the exothermic peak (693 K) and Zr_2Ni is the main phase after the thermal effect (773 K). These results suggest that during heat-

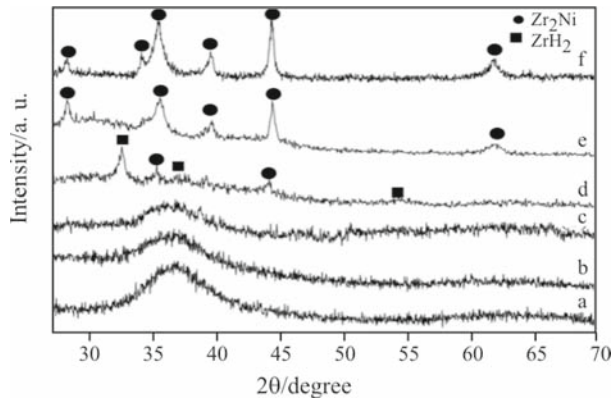

Fig. 5 XRD patterns of a – H-free, b – H-charged, c – H-charged and then annealed up to 663 K, d – H-charged and annealed up to 693 K and e – up to 773 K; f – H-free, annealed up to 773 K

ing ZrH_2 decomposes to hydrogen and zirconium, which then interacts with Ni to form Zr_2Ni. The onset of the exothermic effect corresponds to the high-temperature mass decrease, observed by TG (Fig. 6), giving additional proof for the mechanism proposed. It is important to be underlined that heating up to 663 K of the hydrogenated sample does not result in noticeable microstructural changes, i.e. the alloy remains generally amorphous, Fig. 5.

On the basis of the results obtained in the present study the following mechanism for the hydrogen sorption process and the influence of the hydrogen absorbed on the phase transformations in amorphous $(Co,Ni,Fe)_{33}Zr_{67}$ alloys can be proposed. Small amount of hydrogen absorbed into the amorphous alloys most probably forms a solid solution of hydrogen into the amorphous metal matrix. As a result the thermal stability of the hydrogenated amorphous alloys slightly reduces. The hydrogen first occupies the sites of higher energy levels in the amorphous structure and therefore a very small amount of hydrogen desorbs at low temperature (Fig. 6, curve a). Increasing the hydrogen concentration in the amorphous matrix sites with lower energy are occupied as well and as a result an intense low temperature desorption process can be registered (Fig. 6, curve b). The hydrogen, occupying the trapping sites with lower binding energies, releases during annealing in the temperature range of 440–640 K, well below the crystallization temperatures of the alloys. As a result of the large variety of interstitials with different energy occupied by hydrogen the desorption process in amorphous materials takes place in a wide temperature range (440–640 K), expressed as a broad multi-step effect in the TG hydrogen desorption curve (Fig. 3a) and in the DSC curves (Fig. 4c, inset). Below certain hydrogen concentrations into the alloys the crystallization reactions themselves are not drastically influenced by the hydrogen absorbed, only a decrease in the thermal stability and enthalpy of crystallization is detected. At higher hydrogen concentrations in the amorphous alloys clusters (or nuclei) of ZrH_x are most probably formed, which are small enough and can not be identified by XRD. During heating partial desorption of hydrogen occurs (Fig. 6) and the rest of it is stronger bonded to Zr, the element with high affinity to hydrogen. At present it is not clear whether these clusters form at room temperature or during annealing the hydrogenated sample. Increasing the temperature of annealing these ZrH_x clusters (nuclei) grow and reach a nanometric size. In this way just before the exothermic DSC peak at 713 K nanocrystallites with an average size of 15 nm can be identified by XRD (Fig. 5). Crystallization reaction was not registered by DSC (Fig. 4a). Only when the decomposition of the

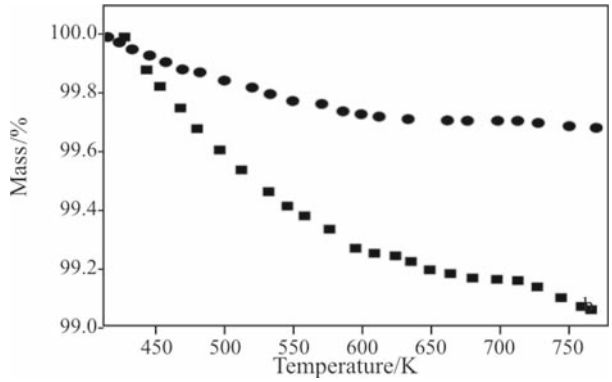

Fig. 6 Hydrogen desorption of $Ni_{33}Zr_{67}$ charged with two different hydrogen concentrations

ZrH_x starts (at about 713 K) formation of the Zr_2Ni proceeds. The last two reactions, taking place simultaneously, result into the DSC exothermic effect in the temperature range of 708–718 K (Fig. 4a). It is important to point out that the Zr_2Ni phase, obtained by annealing the hydrogenated amorphous alloy, has finer nanostructure (~15 nm) than that formed by crystallizing the H-free amorphous material (~21 nm).

Conclusions

Melt-spun amorphous $TM_{33}Zr_{67}$ (*TM*=Fe, Co, Ni) alloys were found to dissolve hydrogen in relatively large amounts in amorphous state. The lower energy bonded hydrogen, dissolved into the amorphous alloys, desorbs during heating in the temperature range of 440–640 K, which is below their crystallization temperatures. During annealing of hydrogen charged amorphous alloy a hydride phase (ZrH_2) is formed. During heating the hydride decomposes at about 713 K and formation of Zr_2Ni takes place in $Ni_{33}Zr_{67}$. The microstructure of the Zr_2Ni crystallized from the H-charged alloy is finer compared to that of the material crystallized from the H-free amorphous alloy, providing an opportunity for the synthesis of nanostructured alloys with refined microstructure.

Acknowledgements

The work has been supported by the Bulgarian Scientific Research Fund under grant BYX-14/05 and by the National Science Fund, Project 'University research center on nanotechnologies and new materials'.

References

1 D. A. Menzel, A. Niklas and U. Köster, Mater. Sci. Eng., A133 (1991) 321.

2 R. Dunlap, G. Stroink, Z. Stadnik and K. Dini, Mater. Sci. Eng., 99 (1988) 543.
3 K. Cho, C. H. Hwang, C. S. Pak and Y. J. Ryeom, J. Less-Common Metals, 89 (1983) 2238.
4 T. Spassov and G. Tzolova, Cryst. Res. Technol., 29 (1994) 99.
5 T. Spassov and U. Köster, J. Mater. Sci., 28 (1993) 2789.
6 U. Koester, T. Spassov and M. Sutton, Proc. III[rd] International Conference on Non-crystalline Solids, Matalascanas, 1991, A.Conde, C. F. Conde and M. Millan, Eds, Spain, pp. 149–152.
7 T. Spassov and U. Köster, Key Eng. Mater., 81–83 (1993) 249.
8 T. Spassov, V. Petkov and U. Köster, Proc. of the IXth Int. Conference on Rapidly Quenched and Metastable Materials, P. Duhaj, P. Mravko and P. Svec, Eds, Bratislava 1996, Elsevier 1997, pp. 224–227.
9 A. Gebert, N. Ismail, U. Wolff, M. Eckert and L. Schultz, J. Intermetallics, 10 (2002) 1207.
10 A. Nobile, W. C. Mosley, J. C. Holder and K. N. Brooks, J. Alloys Compd., 206 (1994) 83.
11 V. A. Yartys, H. Fjellvag, B. C. Hauback and A. B. Riabov, J. Alloys Compd., 274 (1998) 217.
12 V. A. Yartys, H. Fjellvag, I. R. Harris, B. C. Hauback, A. B. Riabov, M. H. Sorby and I. Yu. Zavaliy, J. Alloys Compd., 293–295 (1999) 74.
13 A. M. Viano, P. C. Gibbons and K. F. Kelton, Bull. Am. Phys. Soc., 38 (1993) 681.
14 U. Koester, J. Meinhardt, S. Roos and H. Libertz, Appl. Phys. Lett., 69 (1996) 179.
15 E. Tal-Gutelmacher, N. Eliaz and D. Eliezer, Scripta Materialia, 52 (2005) 777.
16 Y. Arita, T. Ogawa, B. Tsuchiya and T. Matsui, J. Therm. Anal. Cal., 92 (2008) 403.
17 T. Spassov, G. Stergioudis, G. Ivanov and E. K. Polychroniadis, Z. Metallkunde, 89 (1998) 23.
18 S. B. Rybalkaa, V. A. Goltsov, V. A. Didus and D. Fruchart, J. Alloys Compd., 356–357 (2003) 390.
19 T. Spassov, Annuaire de l'Université de Sofia, 88 (1995) 123.
20 J. H. Harris, W. A. Curtin and M. Tenhover, Phys. Rev. B, 36 (1997) 5984.
21 V. Rangelova, T. Spassov and N. Neykov, J. Therm. Anal. Cal., 75 (2004) 373.

Received: December 5, 2007
Accepted: August 13, 2008
Online First: January 12, 2009

DOI: 10.1007/s10973-007-8585-7